Dunham's[7] observations, U_j/U is used in the comparison shown in Fig. 5.

Conclusions

The laminar theory shows that the momentum coefficient is an appropriate jet parameter for moderate values of h/R and U_j/U is appropriate for larger values. This is borne out by the experiments. The theory also shows that the effect of the upstream boundary layer is important for small h/δ and is most significant for smaller values of the jet speed. As the slot height approaches the boundary-layer thickness, this effect becomes negligible. The upstream boundary layer reduces the effectiveness of the jet in providing circulation control.

The theory shows also that the effectiveness of the jet is increased as the slot location is moved downstream. Dunham[7] warns, however, that this effectiveness is lost if the boundary layer on the cylinder separates before the slot is reached.

References

[1] Pai, S. I. and Hsieh, T. Y., "Numerical Solution of Laminar Jet Mixing with and without Free Stream," TN BN-627, 1969, Institute for Fluid Dynamics and Applied Mathematics, Univ. of Maryland.

[2] Kleinstein, G., "Slot Cooling at High Speed Flow," Rept. 68-0141, 1968, Aeronautical Research Lab. Wright-Patterson Air Force Base, Ohio.

[3] Schetz, J. A. and Jannone, J., "Initial Boundary Layer Effects on Laminar Flows with Wall Slot Injection," *Journal of Heat Transfer*, Vol. 87, No. 1, 1965, pp. 157–160.

[4] Dunham, J., "A Tentative Theory of Circulation Control Applied to a Circular Cylinder," Rept. 27-170, 1965, Aeronautical Research Council, England.

[5] Kind, R. J., "A Calculation Method for Circulation Control by Tangential Blowing Around a Bluff Trailing Edge," *Aeronautical Quarterly*, Vol. XIX, Pt. 3, 1968, pp. 205–223.

[6] Flügge-Lotz, I. and Blottner, F. G., "Finite-Difference Computation of the Boundary Layer with Displacement Thickness Interaction," *Journal de Mecanique*, Vol. 2, 1963, pp. 397–423.

[7] Dunham, J., "Experiments Towards a Circulation-Controlled Lifting Rotor. Part I—Wind Tunnel Tests," *Aeronautical Journal of the Royal Aeronautical Society*, Vol. 74, No. 709, 1970, pp. 91–103.

[8] Cheeseman, I. C., "Circulation Control and its Application to Stopped Rotor Aircraft," *Aeronautical Journal of the Royal Aeronautical Society*, Vol. 72, No. 691, 1968, pp. 635–646S.

Stress Redistribution and Instability of Rotating Beams and Disks

E. J. BRUNELLE*

Rensselaer Polytechnic Institute, Troy, N. Y.

Introduction

THIS Note reports the existence of a static inertio-elastic instability of rotating beams and disks that has been previously unnoticed. The instability is not the critical case (yielding occurs first) for rotating structures made of the usual metals but is of primary importance in rotating structures made of low-modulus, high-yield strength materials, such as some plastic materials. Hence, there may be applications of this work for example to tethered space stations and centrifugally stiffened plastic film helicopter rotors. The instability has been unnoticed because in previous analyses the centrifugal force has been assumed to be $m\Omega^2 r$ (for the beam) rather than the actual value of $m\Omega^2(r + u)$, where m is the mass per unit length, Ω is the rotational speed, r is the initial undeformed radius, and u is the radial displacement. A corollary effect of this problem is that there is a stress-redistribution along the radius of the beam or disk due to the inclusion of the $\rho\Omega^2 u$ term at all values of Ω below the critical value. The analysis is given in the following two sections.

Received November 24, 1970.

* Associate Professor of Aeronautics and Astronautics. Member AIAA.

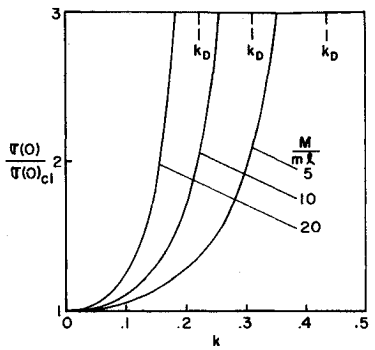

Fig. 1 Root stress ratio $\sigma(0)/\sigma\ (0)_{cl}$ vs rotational parameter.

Rotating Beam with Tip Mass

From elementary considerations the steady-state equation of motion is given by

$$m\Omega^2 l^2(u + l\xi) + (EAu')' = 0 \tag{1}$$

where primes denote differentiation with respect to the nondimensional radial distance ξ(i.e., $0 \leq \xi \leq 1$). For a cantilevered beam with a tip mass M at the free end, the boundary conditions are $u(0) = 0$ and $u'(1) = (Ml/AE)\Omega^2[l + u(1)]$. Applications of the boundary conditions to the solution of Eq. (1) yields the results that the displacement and the stress are given by

$$u(\xi) = l(\{\sin k\xi/[k\cos k(1 - [M/ml]k\tan k)]\} - \xi) \tag{2}$$

$$\sigma(\xi) = E(\{\cos k\xi/[\cos k(1 - [M/ml]k\tan k)]\} - 1) \tag{3}$$

where

$$k^2 = ml^2\Omega^2/EA$$

The classical values of $u(\xi)$ and $\sigma(\xi)$, for comparison, are given by

$$u(\xi)_{cl} = k^2 l[M/ml(6 - k^2) + 3 - \xi^2]\xi/6 \tag{4}$$

$$\sigma(\xi)_{cl} = Ek^2[M/ml(6 - k^2) + 3 - 3\xi^2]/6 \tag{5}$$

It is noticed that Eqs. (2) and (3) possess instabilities when

$$k\tan k = ml/M \tag{6}$$

and that Eqs. (4) and (5) possess no instabilities.

Table 1 K_D vs ml/M

ml/M	k_D
0	0
0.05	0.222
0.10	0.311
0.20	0.433
0.30	0.522
0.40	0.593
0.50	0.653
0.60	0.705
0.70	0.751
0.80	0.791
0.90	0.827
1.00	0.860
.	.
.	.
.	.
∞	1.571

The solution of Eq. (6) for a given ml/M is denoted as k_D. Table 1 presents values of k_D for given ml/M, and Fig. 1 plots $\sigma(0)/\sigma(0)_{cl}$ for a wide range of k.

Rotating Disk

The appropriate equations are

$$\rho\Omega^2(r + u) + d\sigma_r/dr + (\sigma_r - \sigma_\theta)/r = 0 \quad (7)$$

$$\epsilon_r = du/dr = (\sigma_r - \nu\sigma_\theta)/E \quad (8)$$

$$\epsilon_\theta = u/r = (\sigma_\theta - \nu\sigma_r)/E \quad (9)$$

Inverting Eqs. (8) and (9) and substituting the results into Eq. (7) yields the displacement equilibrium equation

$$r^2d^2u/dr^2 + rdu/dr + [\Omega_*{}^2(r/b)^2 - 1]u = \Omega_*{}^2r^3/b^2 \quad (10)$$

where

$$\Omega_*{}^2 = (1 - \nu^2)\rho\Omega^2b^2/E \quad (11)$$

The general solution for u, σ_r, and σ_θ are then given by

$$u/b = AJ_1(\Omega_*r/b) + BY_1(\Omega_*r/b) - (r/b) \quad (12)$$

$$(1 - \nu^2)\sigma_r/E = A[\Omega_*J_0(\Omega_*r/b) - (b/r)(1 - \nu)J_1(\Omega_*r/b)] + B[\Omega_*Y_0(\Omega_*r/b) - (b/r)(1 - \nu)Y_1(\Omega_*r/b)] - (1 + \nu) \quad (13)$$

$$(1 - \nu^2)\sigma_\theta/E = A[(b/r)(1 - \nu)J_1(\Omega_*r/b) + \nu\Omega_*J_0(\Omega_*r/b)] + B[(b/r)(1 - \nu)Y_1(\Omega_*r/b) + \nu\Omega_*Y_0(\Omega_*r/b)] - (1 + \nu) \quad (14)$$

Applying the boundary conditions $u(a) = \sigma_r(b) = 0$ yields for A and B,

$$A = [(1 + \nu)Y_1(\Omega_*a/b) - (a/b)\Omega_*Y_0(\Omega_*) + (a/b)(1 - \nu)Y_1(\Omega_*)]/C \quad (15)$$

$$B = [(a/b)\Omega^*J_0(\Omega^*) - (a/b)(1 - \nu)J_1(\Omega^*) - (1 + \nu)J_1(\Omega_*a/b)]/C \quad (16)$$

where

$$C = Y_1(\Omega_*a/b)[\Omega_*J_0(\Omega_*) - (1 - \nu)J_1(\Omega_*)] + J_1(\Omega_*a/b)[(1 - \nu)Y_1(\Omega_*) - \Omega_*Y_0(\Omega_*)] \quad (17)$$

The Ω_* at which the instability occurs is given by $C = 0$ and is denoted by Ω_{*D}. These values are given in Table 2 for $\nu = 0.3$ and various a/b ratios. The corresponding classical results are given by

$$(u/b)_{cl} = A_*r/b + B_*b/r - \Omega_*{}^2(r/b)^3/8 \quad (18)$$

$$(1 - \nu^2)(\sigma_r)_{cl}/E = A_*(1 + \nu) - B_*(b/r)^2(1 - \nu) - \Omega_*{}^2(r/b)^2(3 + \nu)/8 \quad (19)$$

$$(1 - \nu^2)(\sigma_\theta)_{cl}/E = A_*(1 + \nu) + B_*(b/r)^2(1 - \nu) - \Omega_*{}^2(r/b)^2(1 + 3\nu)/8 \quad (20)$$

and applying the boundary conditions $u_r(a)_{cl} = \sigma_r(b)_{cl} = 0$ yields

$$A_* = \Omega_*{}^2[(a/b)^4(1 - \nu) + (3 + \nu)]/8C_* \quad (21)$$

$$B_* = \Omega_*{}^2[(a/b)^4(1 + \nu) - (a/b)^2(3 + \nu)]/8C_* \quad (22)$$

Table 2 Ω_{*D} vs a/b for $\nu = 0.3$

$\nu = 0.3$	
a/b	Ω_{*D}
0.10	2.088
0.30	2.404
0.50	3.183
0.70	5.194
0.90	15.605

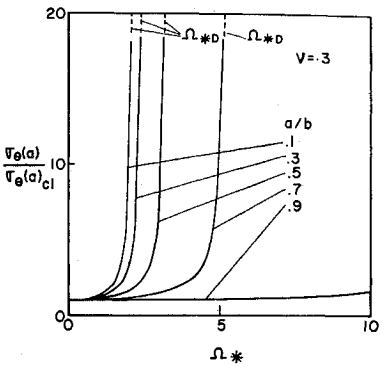

Fig. 2 Tangential hoop stress ratio $\sigma\theta(a)/\sigma\theta(a)_{cl}$ vs rotational parameter Ω^*.

where

$$C_* = (a/b)^2(1 - \nu) + (1 + \nu) \quad (23)$$

It is noted that no instability is present in the classical results.

Preliminary investigation showed that $\sigma_\theta(a)$ is still the largest stress (as it is in the classical case) so the important result is the ratio $\sigma_\theta(a)/\sigma_\theta(a)_{cl}$ plotted vs Ω_* for various a/b ratios. These results are shown in Fig. 2.

Discussion

The preceeding two problems have been analyzed assuming linear elastic behavior. It is to be noted that if the material used has a nonlinear softening behavior† the instability will still exist and in fact will occur at a much lower rotational speed.

† i.e. strain hardening material.

Streamwise Vortices in Reattaching High-Speed Flows: A Suggested Approach

JEAN J. GINOUX*
von Kármán Institute, Belgium

THERE is experimental evidence of the systematic development of streamwise vortices in reattaching two-dimensional supersonic flows. They have a remarkable periodicity with a wavelength equal to two to three times the

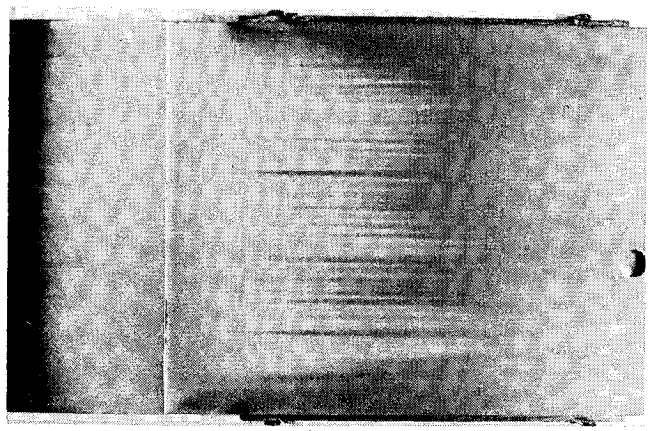

Fig. 1 Spanwise variation of skin friction for $M = 5.3$ flow over a backward facing step.

Received December 15, 1970.

* Professor at Brussels University and Head of the High Speed Laboratory at the von Kármán Institute.